CHEMISTRY OF MATERIALS
Article

Chem. Mater. **2010,** *22,* 2653–2661 2653
DOI:10.1021/cm100107p

How Processing Atmosphere Influences the Evolution of GeO_2-Embedded Germanium Nanocrystals Obtained from the Thermolysis of Phenyl Trichlorogermane-Derived Polymers

Eric J. Henderson, Colin M. Hessel,† Ronald G. Cavell, and Jonathan G.C. Veinot*

Department of Chemistry, University of Alberta, Edmonton, Alberta, Canada. †*Current address: University of Texas at Austin, Chemical Engineering, 1 University Station C0400, CPE 4.464 Austin, TX 78712.*

Received January 12, 2010. Revised Manuscript Received February 26, 2010

We report the influence of processing atmosphere on the evolution of oxide-embedded germanium nanocrystals (Ge-NCs) formed by the thermal processing of $(C_6H_5GeO_{1.5})_n$ sol−gel polymers. In an inert processing atmosphere (100% Ar), the generation of elemental Ge from thermally induced disproportionation of the germanium rich oxide (GRO) leads to GeO_2-embedded Ge-NCs whose size is independent of peak processing temperature and time. Processing in a slightly reducing atmosphere (5% H_2/95% Ar) activates a second Ge-NC formation and growth pathway, involving the reduction of Ge oxide species. Here, we report that the processing atmosphere governs the distribution of Ge species. By modifying the contributions from redistribution and reduction reactions within the GRO, diffusion of Ge atoms throughout the oxide matrix and formation and growth of Ge-NCs are impacted.

Introduction

Group 14 semiconductor nanostructures have generated great excitement and received much attention over the past several decades, largely due to their unique optical and electronic properties. Spurred by the possibility and recent realization[1,2] of silicon-based optoelectronic applications following the discovery of efficient visible photoluminescence (PL) from silicon nanocrystals (Si-NCs),[3] numerous preparative methods for Si-NCs have since emerged. The demonstration of different Si-NC architectures, including oxide-embedded,[4,5] polymer-encapsulated,[6,7] and freestanding particles,[8] coupled with intense research into their optical and electronic properties, has expanded the possible applications for Si-NCs to include nonvolatile memory,[9,10] photovoltaics,[6] and biological fluorescence imaging,[11] among others. Driven by the early successes for Si-NCs, recent research has increasingly focused on Ge nanostructures. These systems are beginning to exhibit distinct advantages over their Si counterparts including higher carrier mobility[12] and more pronounced quantum confinement effects,[13] as well as improved data retention and write/erase speeds for nonvolatile memory applications.[14−16]

It is well established that quantum size effects play a significant role in altering the optical and electronic properties of semiconductor nanocrystals, including Ge.[17] Although these effects are exploited in nanocrystal size-tuned PL, their influence can also be detrimental, causing inhomogeneous broadening in emission spectra[18,19] and affecting charging characteristics.[20] In this regard, the realization of well-defined germanium nanocrystals (Ge-NCs) with predictable characteristics will surely contribute to the fundamental and comprehensive understanding of these quantum-size effects and their macroscopic manifestations. In addition, the development

*To whom correspondence should be addressed. Fax: 780-492-8231. Tel: 780-492-7206. E-mail: jveinot@ualberta.ca.

(1) Pavesi, L.; Dal Negro, L.; Mazzoleni, C.; Franzò, G.; Priolo, F. *Nature* **2000**, *408*, 440.
(2) Walters, R. J.; Bourianoff, G. I.; Atwater, H. A. *Nat. Mater.* **2005**, *4*, 143.
(3) Canham, L. T. *Appl. Phys. Lett.* **1990**, *57*, 1046.
(4) Hessel, C. M.; Henderson, E. J.; Veinot, J. G. C. *Chem. Mater.* **2006**, *18*, 6139.
(5) Hessel, C. M.; Henderson, E. J.; Veinot, J. G. C. *J. Phys. Chem. C* **2007**, *111*, 6956.
(6) Kortshagen, U.; Anthony, R.; Gresback, R.; Holman, Z.; Ligman, R.; Liu, C. Y.; Mangolini, L.; Campbell, S. A. *Pure Appl. Chem.* **2008**, *80*, 1901.
(7) Li, Z. F.; Swihart, M. T.; Ruckenstein, E. *Langmuir* **2004**, *20*, 1963.
(8) Veinot, J. G. C. *Chem. Commun.* **2006**, 4160.
(9) Lombardo, S.; De Salvo, B.; Gerardi, C.; Baron, T. *Microelectron. Eng.* **2004**, *72*, 388.
(10) Compagnoni, C. M.; Gusmeroli, R.; Ielmini, D.; Spinelli, A. S.; Lacaita, A. L. *J. Nanosci. Nanotech.* **2007**, *7*, 193.
(11) Erogbogbo, F.; Yong, K. T.; Roy, I.; Xu, G. X.; Prasad, P. N.; Swihart, M. T. *ACS Nano* **2008**, *2*, 873.
(12) Brunco, D. P.; De Jaeger, B.; Eneman, G.; Satta, A.; Terzieva, V.; Souriau, L.; Leys, F. E.; Pourtois, G.; Houssa, M.; Opsomer, K.; Nicholas, G.; Meuris, M.; Heyns, M. M. *ECS Trans.* **2007**, *11*, 479.
(13) Heath, J. R.; Shiang, J. J.; Alivisatos, A. P. *J. Chem. Phys.* **1994**, *101*, 1607.
(14) Kanoun, M.; Busseret, C.; Poncet, A.; Souifi, A.; Baron, T.; Gautier, E. *Solid-State Electron.* **2006**, *50*, 1310.
(15) Batra, Y.; Kabiraj, D.; Kanjilal, D. *Solid State Commun.* **2007**, *143*, 213.
(16) Beyer, V.; von Borany, J.; Klimenkov, M. *J. Appl. Phys.* **2007**, *101*, 094507.
(17) Bostedt, C.; Van Buuren, T.; Willey, T. M.; Franco, N.; Terminello, L. J.; Heske, C.; Möller, T. *Appl. Phys. Lett.* **2004**, *84*, 4056.
(18) Sychugov, I.; Juhasz, R.; Galeckas, A.; Valenta, J.; Linnros, J. *Optical Mater.* **2005**, *27*, 973.
(19) Alivisatos, A. P. *J. Phys. Chem.* **1996**, *100*, 13226.
(20) El Hdiy, A.; Gacem, K.; Troyon, M.; Ronda, A.; Bassani, F.; Berbezier, I. *J. Appl. Phys.* **2008**, *104*, 063716.

Published on Web 03/18/2010

and detailed understanding of synthetic techniques that provide predictable, well-defined nanocrystals with narrow size distributions are necessary if the full potential of Ge-NCs is to be realized and practically implemented into leading-edge applications.

We recently demonstrated near-monodisperse Ge-NCs can be prepared by the thermal processing of $(C_6H_5GeO_{1.5})_n$ sol−gel polymers in a hydrogen-containing atmosphere.[21] These precursors were designed to generate a substoichiometric oxide with a composition approaching "$GeO_{1.5}$" upon thermal decomposition. Reports employing substoichiometric oxides of germanium (GeO_x, $0 \leq x \leq 2$), known as germanium rich oxides (GRO), as Ge-NC precursors are quite sparse throughout the literature.[15,22,23] Analogous silicon rich oxides (SROs) have been studied extensively and are known to be versatile precursors for the generation of oxide embedded Si-NCs. From SROs, Si-NCs are formed exclusively through the disproportionation of SiO_x into elemental Si and the stoichiometric oxide, SiO_2; hydrogen is often used in the processing atmosphere to passivate dangling bonds to improve PL efficiency.[4,5] Similar to their Si-based equivalents, GROs disproportionate with appropriate thermal processing and under suitable conditions yield Ge-NCs embedded in a GeO_2-like matrix.

Although concisely described as an overall disproportionation reaction of the form $4GeO_{1.5} \rightarrow Ge + 3GeO_2$, the thermal transformation of GROs into GeO_2-embedded Ge-NCs involves a series of redistribution reactions as outlined in eq 1. These reactions are analogous to those leading to the formation of Si-NCs from SROs[4,24] and silicon carbide NCs from silicon oxycarbides.[25,26] These reactions are thermodynamically driven by the formation of the stoichiometric oxide (GeO_2) which results in the concomitant production of elemental Ge. Subsequent clustering of Ge atoms and crystallization of domains leads to Ge-NC formation and growth.

$$\begin{aligned} GeO_{3/2} + GeO_{3/2} &\rightarrow GeO_{2/2} + GeO_{4/2} \\ GeO_{3/2} + GeO_{2/2} &\rightarrow GeO_{1/2} + GeO_{4/2} \\ GeO_{3/2} + GeO_{1/2} &\rightarrow Ge + GeO_{4/2} \end{aligned} \quad (1)$$

In the presence of H_2, the various Ge oxide species (i.e., $GeO_{4/2}$, $GeO_{3/2}$, $GeO_{2/2}$, $GeO_{1/2}$) are susceptible to chemical reduction (eq 2). As a result, additional elemental Ge is available and can contribute to the formation and growth of Ge-NCs.[27−29] This additional NC growth pathway presents a substantial difference in the thermal behavior of GROs compared to SROs, in which the reduction of SiO_2 by atmospheric H_2 is not possible at typical processing temperatures of ca. 800−1400 °C.

$$\begin{aligned} GeO_{4/2} + H_2 &\rightarrow GeO_{2/2} + H_2O \\ GeO_{3/2} + H_2 &\rightarrow GeO_{1/2} + H_2O \\ GeO_{2/2} + H_2 &\rightarrow Ge + H_2O \\ 2GeO_{1/2} + H_2 &\rightarrow 2Ge + H_2O \end{aligned} \quad (2)$$

Modulating the relative contributions of the reactions summarized in eqs 1 and 2 will certainly have a dramatic impact on the evolution of Ge-NCs from GROs. Recent investigations of SiO_2-embedded Ge-NCs produced via thermal processing of cosputtered SiO_2−Ge films have shown processing atmosphere affects nanocrystal formation pathways.[27,29] Specifically, films prepared in a slightly reducing atmosphere (10% H_2/90% N_2) showed Ge nanodomain crystallization at lower temperatures compared to samples processed in inert conditions and led to the production of smaller Ge-NCs. The authors proposed reduction of the Ge oxide species decreased the energetic barrier to nanocrystal nucleation by increasing the concentration of elemental Ge and allowing greater diffusion of Ge atoms throughout the matrix by forming network modifying hydroxyl (−OH) groups which "open-up" the solid matrix network. Similar arguments have been proposed for the precipitation of Ge clusters during the reduction of $Si_{1-x}Ge_xO_2$.[30] In contrast to these examples of SiO_2-embedded Ge-NCs, in which the reduction of minor Si−O−Ge species by the H_2-containing atmosphere could participate in Ge-NC formation, a GeO_2 matrix provides a comparatively unlimited Ge feedstock to nanocrystal formation and growth under similar conditions. To our knowledge, there have been no reports outlining the influence of processing atmosphere on the evolution of GeO_2-embedded Ge-NCs.

In this work, we investigate the atmospheric dependence of Ge-NC formation and growth from thermal processing of $(C_6H_5GeO_{1.5})_n$ condensation polymers by uncoupling the disproportionation and reduction NC formation pathways. Eliminating the contribution of the Ge oxide reduction route (eq 2) by processing in an inert atmosphere allows an independent investigation of the disproportionation mechanism. The formation and growth of the oxide-embedded Ge-NCs described herein were evaluated as a function of thermal processing time and temperature in inert atmosphere (100% Ar) and were directly compared to those obtained from processing in a slightly reducing atmosphere (5% H_2/95% Ar). These materials were characterized using thermogravimetric analysis (TGA), near-edge X-ray absorption fine structure (NEXAFS) spectroscopy, X-ray photoelectron spectroscopy (XPS), and X-ray diffraction (XRD).

(21) Henderson, E. J.; Hessel, C. M.; Veinot, J. G. C. *J. Am. Chem. Soc.* **2008**, *130*, 3624.
(22) Zacharias, M.; Bläsing, J.; Löhmann, M.; Christen, J. *Thin Solid Films* **1996**, *278*, 32.
(23) Ardyanian, M.; Rinnert, H.; Devaux, X.; Vergnat, M. *Appl. Phys. Lett.* **2006**, *89*, 011902.
(24) Belot, V.; Corriu, R.; Leclercq, D.; Mutin, P. H.; Vioux, A. *Chem. Mater.* **1991**, *3*, 127.
(25) Burns, G. T.; Taylor, R. B.; Xu, Y.; Zangvil, A.; Zank, G. A. *Chem. Mater.* **1992**, *4*, 1313.
(26) Henderson, E. J.; Veinot, J. G. C. *J. Am. Chem. Soc.* **2009**, *131*, 809.
(27) Choi, W. K.; Chew, H. G.; Zheng, F.; Chim, W. K.; Foo, Y. L.; Fitzgerald, E. A. *Appl. Phys. Lett.* **2006**, *89*, 113126.
(28) Paine, D. C.; Caragianis, C.; Kim, T. Y.; Shigesato, Y.; Ishahara, T. *Appl. Phys. Lett.* **1993**, *62*, 2842.
(29) Chew, H. G.; Zheng, F.; Choi, W. K.; Chim, W. K.; Foo, Y. L.; Fitzgerald, E. A. *Nanotechnology* **2007**, *18*, 065302.
(30) Caragianis-Broadbridge, C.; Blaser, J. M.; Paine, D. C. *J. Appl. Phys.* **1997**, *82*, 1626.

Experimental Section

Reagents and Materials. Phenyl trichlorogermane ($C_6H_5GeCl_3$, 98%) was purchased from Sigma Aldrich and stored in a nitrogen glovebox in subdued light. Isopropyl alcohol (IPA, ≥99.5%) was purchased from Fisher Scientific. All reagents were used as received. High-purity deionized (DI) water (18.2 MΩ/cm) was obtained from a Barnstead Nanopure Diamond purification system. Ground Ge wafers (Evergreen Semiconductor, San Jose, CA) and GeO_2 powder (Aldrich) were used as NEXAFS standards.

$(C_6H_5GeO_{1.5})_n$ Condensation Polymer Preparation. In a typical synthesis, 16 mL of a 65% (v/v) solution of IPA in DI water was added dropwise to 4.5 mL of $C_6H_5GeCl_3$ (7.13 g, 27.8 mmol) under Ar atmosphere with vigorous stirring, using standard Schlenk techniques. The clear and colorless $C_6H_5GeCl_3$ immediately turned cloudy white as the aqueous IPA solution was added. Hydrolysis of the precursor was confirmed through monitoring the pH of the reaction mixture (pH = 1). The cloudy white mixture was gently heated at 60 °C and stirred for 24 h to ensure complete condensation. The resulting white solid precipitate was isolated by vacuum filtration, washed three times with DI water, and dried in vacuo. The white solid product was obtained in yields greater than 90% and is stable under ambient conditions.

Ge-NC/GeO_2 Composite Preparation. $(C_6H_5GeO_{1.5})_n$ condensation polymer was placed in a quartz reaction boat and transferred to a high-temperature tube furnace. Samples were heated to defined peak processing temperatures at 18 °C/min for predetermined times, either under slightly reducing (5% H_2/95% Ar) or inert (100% Ar) atmospheres. After cooling to room temperature, the solid materials were mechanically ground in an agate mortar and pestle into fine, free-flowing powders.

Thermogravimetric Analysis (TGA). TGA was performed using a Perkin-Elmer Pyris 1 TGA equipped with Pyris Thermal Analysis 7.0 software. $(C_6H_5GeO_{1.5})_n$ condensation polymer samples were placed in a platinum pan and heated in 5% H_2/95% Ar or 100% Ar from room temperature to 900 °C at 20 °C/min.

Near-Edge X-ray Absorption Fine Structure (NEXAFS) Spectroscopy. The 20-BM-B: Sector 20-Bending Magnet Beamline of the PNC/XOR facilities at the Advanced Photon Source (APS) at Argonne National Laboratory provided highly monochromatic X-rays for NEXAFS spectroscopic analysis. The photon flux at the Ge K-edge (11103 eV) was ca. 2×10^8 photons/s, and the resolution was greater than 1 eV. The high resolution was provided by a Si (111) double crystal monochromator with Rh-coated harmonic rejection mirror set to 4 mrad placed before the entrance slits. X-ray absorption spectra were measured in transmittance mode by monitoring the photon flux through in-line ionization chambers (N_2, 1 atm) placed before the sample (I_0), between the sample and reference (I_1), and after the reference (I_{ref}). All spectra were collected with step sizes of 0.3 eV through the edge. All oxide-embedded Ge-NC samples were freshly ground and mounted on Kapton tape prior to analysis. NEXAFS spectra were calibrated to a GeO_2 reference foil by setting the first derivative maximum of the Ge K-edge absorption to 11111.03 eV. All spectra were processed with ATHENA software.[31]

X-ray Photoelectron Spectroscopy (XPS). XPS was performed at the Alberta Centre for Surface Engineering and Science (ACSES) using a Kratos Axis Ultra instrument operating in energy spectrum mode at 210 W. The base pressure and operating chamber pressure were maintained at $\leq 10^{-7}$ Pa. A monochromatic Al Kα source (λ = 8.34 Å) was used to irradiate the samples, and the spectra were obtained with an electron takeoff angle of 90°. To control sample charging, the charge neutralizer filament was used during all experiments. Wide survey spectra were collected using an elliptical spot with 2 and 1 mm major and minor axis lengths, respectively, and a 160 eV pass energy with a step of 0.33 eV. CasaXPS (Vamas) software was used to process high-resolution spectra. The Ge 3d photoelectron peak exhibits a $3d_{5/2}$ and Ge $3d_{3/2}$ spin−orbit splitting of 0.585 eV with an intensity ratio of 0.58.[32,33] All spectra were calibrated to the C 1s emission (284.8 eV). After calibration, the background from each spectrum was subtracted using a Shirley-type background to remove most of the extrinsic loss structure.

X-ray Powder Diffraction (XRD). XRD was performed using an INEL XRG 3000 X-ray diffractometer equipped with a Cu Kα radiation source (λ = 1.54 Å). Bulk crystallinity for all samples was evaluated on finely ground powders mounted on a low-intensity background silicon (100) sample holder.

Results

Thermogravimetric analysis (TGA) was performed on the as-prepared $(C_6H_5GeO_{1.5})_n$ polymer in 5% H_2/95% Ar and 100% Ar to evaluate if processing atmosphere composition influenced the initial pyrolytic decomposition of the precursor. Thermal profiles were identical for samples processed in both atmospheres, exhibiting a total weight loss of ca. 50% (not shown), consistent with near-complete liberation of the phenyl substituents. After residual solvent evaporation (T ≤ 150 °C), the onset of thermal decomposition was 300 °C, in agreement with previous reports of phenyl germane decomposition.[34] Liberation of the phenyl groups was further supported through coupled TGA-IR characterization, which allowed qualitative probing of the reaction byproducts and confirmed the liberation of aromatic fragments. In both processing atmospheres, additional weight loss (ca. 5%) was observed upon heating to higher temperatures (i.e., ≥700 °C) that we attribute to evaporation of elemental Ge. Although this temperature is below the melting point of bulk Ge (938 °C), recent investigations on the size-dependent melting point of oxide-embedded Ge-NCs have reported a melting point depression of as much as 125 K with respect to bulk crystalline Ge (i.e., ca. 800 °C) for NCs of similar sizes to those reported here.[35] Since the behavior of the as-prepared polymer was identical in both processing atmospheres studied, we conclude that processing atmosphere does not have a detectable effect on the initial pyrolytic decomposition of the $(C_6H_5GeO_{1.5})_n$ polymers.

Thermal liberation of the phenyl moieties from $(C_6H_5GeO_{1.5})_n$ leaves an amorphous GRO network that is susceptible to thermally induced redistribution reactions and, under appropriate processing atmosphere,

(31) Ravel, B.; Newville, M. *J. Synchrotron Radiat.* **2005**, *12*, 537.
(32) Schmeisser, D.; Schnell, R. D.; Bogen, A.; Himpsel, F. J.; Rieger, D.; Landgren, G.; Morar, J. F. *Surf. Sci.* **1986**, *172*, 455.
(33) Hanrath, T.; Korgel, B. A. *J. Am. Chem. Soc.* **2004**, *126*, 15466.
(34) Hanrath, T.; Korgel, B. A. *J. Am. Chem. Soc.* **2002**, *124*, 1424.
(35) Lopeandía, A. F.; Rodríguez-Viejo, J. *Thermochim. Acta* **2007**, *461*, 82.

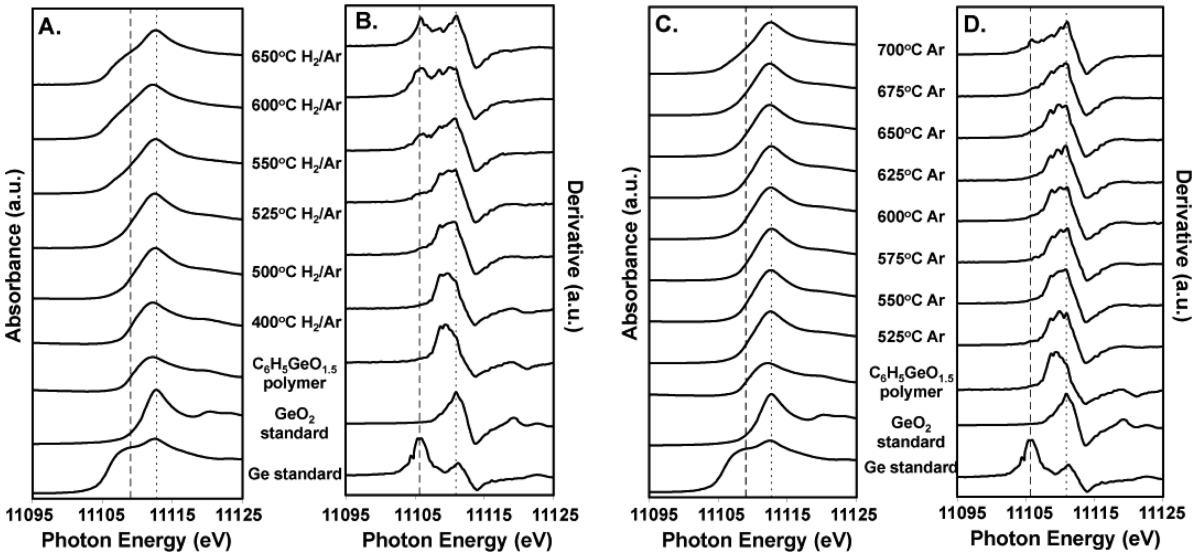

Figure 1. (A) NEXAFS spectra at the Ge K-edge showing the effect of peak thermal processing temperature of $(C_6H_5GeO_{1.5})_n$ for 1 h under 5% H_2/95% Ar. (B) Derivative plot of the NEXAFS spectra. (C) NEXAFS spectra at the Ge K-edge showing the effect of peak thermal processing temperature of $(C_6H_5GeO_{1.5})_n$ for 1 h under 100% Ar. (D) Derivative plot of the NEXAFS spectra. Vertical lines are provided to show the peak energies for Ge (---) and GeO_2 (···) standards.

chemical reduction (see eqs 1 and 2). The relative contributions of these reactions to the overall thermal transformation of the GRO network in different processing atmospheres is effectively demonstrated by monitoring and comparing the evolution of the Ge electronic structure at different stages in the thermal processing by near-edge X-ray absorption fine structure (NEXAFS) spectroscopy. Synchrotron-based NEXAFS spectroscopy has previously proved to be a valuable characterization technique for evaluating Ge nanostructures.[36−38] Comparing NEXAFS spectra of our samples to appropriate standards allows for qualitative identification of different Ge species with high sensitivity, especially elemental Ge and GeO_2.

Figure 1A shows the evolution of the normalized NEXAFS spectra at the Ge K-edge with peak processing temperature for samples of $(C_6H_5GeO_{1.5})_n$ thermally processed in 5% H_2/95% Ar. Prior to thermal treatment, unprocessed $(C_6H_5GeO_{1.5})_n$ is characterized by a NEXAFS spectrum that contains a single absorption feature with a peak energy of 11112.1 eV. When compared to the peak absorption energies of elemental Ge and amorphous GeO_2 standards at 11109.0 and 11113.0 eV, respectively, this intermediate absorption energy is consistent with an empirical formula of $C_6H_5GeO_{1.5}$, owing to the lesser electronic demand from the phenyl substituent on the Ge centers. This observation is also in agreement with spectroscopic investigations reporting that phenyl substituents on Ge are involved in $(p \rightarrow d)\pi$ interactions, further increasing the electron density on the Ge center.[39] These results are further supported by XPS characterization (vide infra).

The evolution of the NEXAFS spectra for $(C_6H_5GeO_{1.5})_n$ thermally processed between 400 and 650 °C in 5% H_2/95% Ar is characterized by a gradual shift of the dominant absorption peak to higher energies and the concomitant emergence and growth of a low energy shoulder (Figure 1A). Specifically, as the processing temperature is increased above 500 °C, the peak absorption at 11112.1 eV gradually shifts to 11113.0 eV, consistent with a transformation toward a GeO_2 oxide environment. Simultaneously, at temperatures above 500 °C, a shoulder emerges at ca. 11109 eV, ascribed to elemental Ge, which grows in intensity with increasing processing temperature. Similar spectral profiles showing absorptions for both elemental Ge and GeO_2 have been reported for other oxide-encapsulated Ge nanostructures.[36] These trends are also evident in the evolution of the derivative plot (Figure 1B), in which the peak maxima correspond to the greatest slopes in the absorption spectra (i.e., $\Delta\mu/\Delta E$), often the midpoint of the absorption edges. These observations are consistent with the formation of elemental Ge and GeO_2 from the GRO network as described in eqs 1 and 2.

The effect of removing the Ge oxide reduction pathway for Ge production (eq 2) can be appreciated by examining Figure 1C, which shows the normalized NEXAFS spectra at the Ge K-edge for samples of $(C_6H_5GeO_{1.5})_n$ thermally processed from 525 to 700 °C under 100% Ar. Samples processed at temperatures below 525 °C are not included as no detectable transformations were observed. When directly compared to data in Figure 1A (i.e., 5% H_2/95% Ar), it is clear a dramatic difference exists in the electronic characteristics of the Ge species at all temperatures evaluated. Although a shift in the absorption peak characterizing the $(C_6H_5GeO_{1.5})_n$ to an energy consistent with GeO_2 (i.e., 11112.1 to 11113.0 eV) is observed at

(36) Sun, X. H.; Didychuk, C.; Sham, T. K.; Wong, N. B. *Nanotechnology* **2006**, *17*, 2925.
(37) Sham, T. K. *Int. J. Nanotech.* **2008**, *5*, 1194.
(38) Daly, B.; Kulkarni, J. S.; Arnold, D. C.; Shaw, M. T.; Nikitenko, S.; Morris, M. A.; Holmes, J. D. *J. Mater. Chem.* **2006**, *16*, 3861.
(39) Whitesides, G. M.; Selgestad, J. G.; Thomas, S. P.; Andrews, D. W.; Morrison, B. A.; Panek, E. J.; San Filippo, J., Jr. *J. Organomet. Chem.* **1970**, *22*, 365.

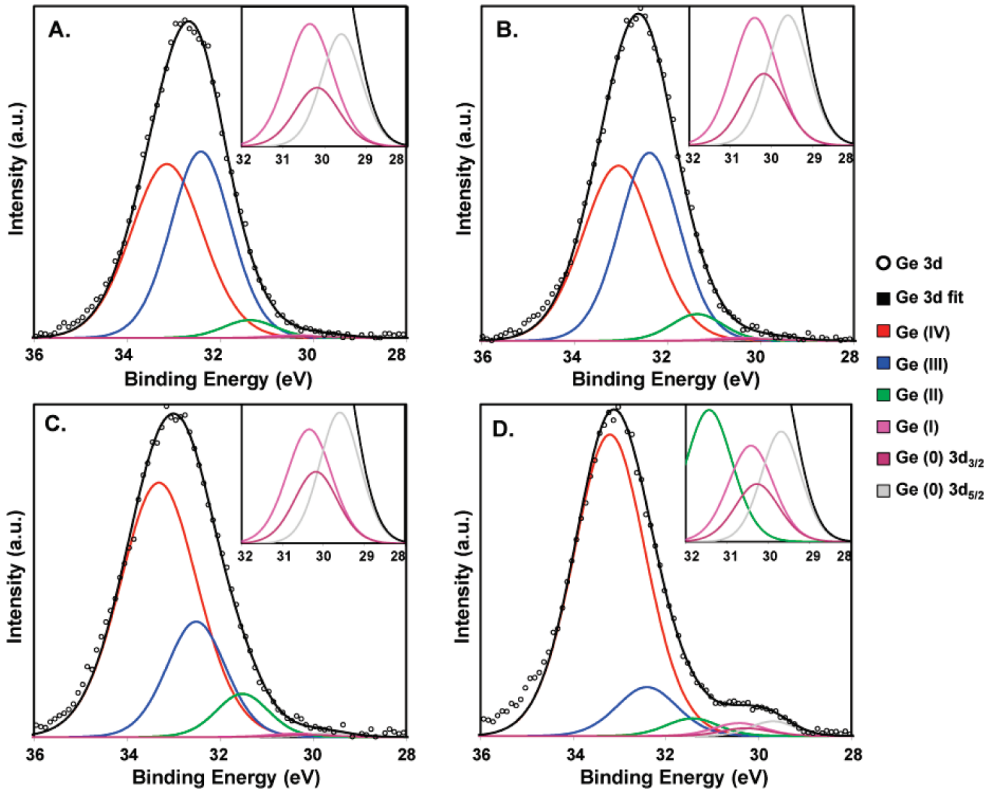

Figure 2. High-resolution XP spectra of the Ge 3d region of $(C_6H_5GeO_{1.5})_n$ thermally processed at (A) 600 °C for 1 h in 100% Ar, (B) 650 °C for 1 h in 100% Ar, (C) 700 °C for 1 h in 100% Ar, and (D) 600 °C for 1 h in 5% H_2/95% Ar. All insets are magnifications of the low-energy region of the associated spectrum.

approximately the same temperature as noted for 5% H_2/95% Ar (i.e., $T > 500$ °C), the emergence of elemental Ge only appears at T ≥ 600 °C, as opposed to 500 °C for the H_2-containing atmosphere. Furthermore, the increase in the intensity of this $Ge^{(0)}$ feature with processing temperature is much less pronounced. These trends are also evident in the derivative plot (Figure 1D).

In a 100% Ar atmosphere, the absence of H_2 precludes any possibility of chemical reduction of Ge oxide species (eq 2). Therefore, the trends depicted in Figure 1C,D arise exclusively from redistribution/disproportionation processes occurring in the GRO network (eq 1). For the present experimental conditions, we draw the following conclusions: (1) the appearance of GeO_2 at $T > 500$ °C indicates that heating to this temperature is necessary to initiate the redistribution chemistry, and (2) the redistribution chemistry produces $Ge^{(0)}$ at T ≥ 600 °C. The temperature difference observed between the onset of network redistribution and the formation of elemental Ge may be reasonably attributed to the energy necessary to overcome atomic diffusion of Ge through the oxide matrix, required for the formation of $Ge^{(0)}$.

In 5% H_2/95% Ar (Figures 1A,B), the appearance of GeO_2 at $T > 500$ °C supports our proposed temperature onset for the redistribution chemistry. However, the emergence of $Ge^{(0)}$ at 525 °C is necessarily due to chemical reduction of Ge oxides (either GeO_2 or other intermediate oxide species) by hydrogen. In addition, we note a greater relative intensity of the $Ge^{(0)}$ spectral feature for H_2-processed samples, consistent with contributions from both the redistribution and reduction pathways. From this data, it is clear that processing atmosphere composition plays a crucial role in the evolution of the GRO network.

To further elucidate the effect of atmospheric composition on the thermal processing of $(C_6H_5GeO_{1.5})_n$, additional information regarding the evolution of the Ge electronic structure and the relative concentrations of the possible intermediate Ge oxide species formed from eqs 1 and 2 were obtained using X-ray photoelectron spectroscopy (XPS). Due to their difference in sample penetration depth, the use of surface sensitive XPS in conjunction with NEXAFS also allows a comparison of surface vs bulk species, an important feature of reactions involving solid and gaseous reactants. The XP spectrum of unprocessed $(C_6H_5GeO_{1.5})_n$ (Supporting Information, Figure S1) is characterized by a single broad emission peak centered at ca. 32.2 eV that is readily fit to Ge $3d_{5/2}$ and Ge $3d_{3/2}$ spin−orbit partner lines. This is in agreement with literature reports of intermediate Ge oxide species.[40]

Figure 2 shows the evolution of the Ge 3d region of the XP spectra for samples of $(C_6H_5GeO_{1.5})_n$ processed for 1 h in 100% Ar at 600 °C (A), 650 °C (B), and 700 °C (C). These samples are characterized by spectra dominated by a broad asymmetric photoemission band centered between 32 and 33 eV with a low energy shoulder. For

(40) Molle, A.; Bhuiyan, M. N. K.; Tallarida, G.; Fanciulli, M. *Mater. Sci. Semicond. Process.* **2006**, *9*, 673.

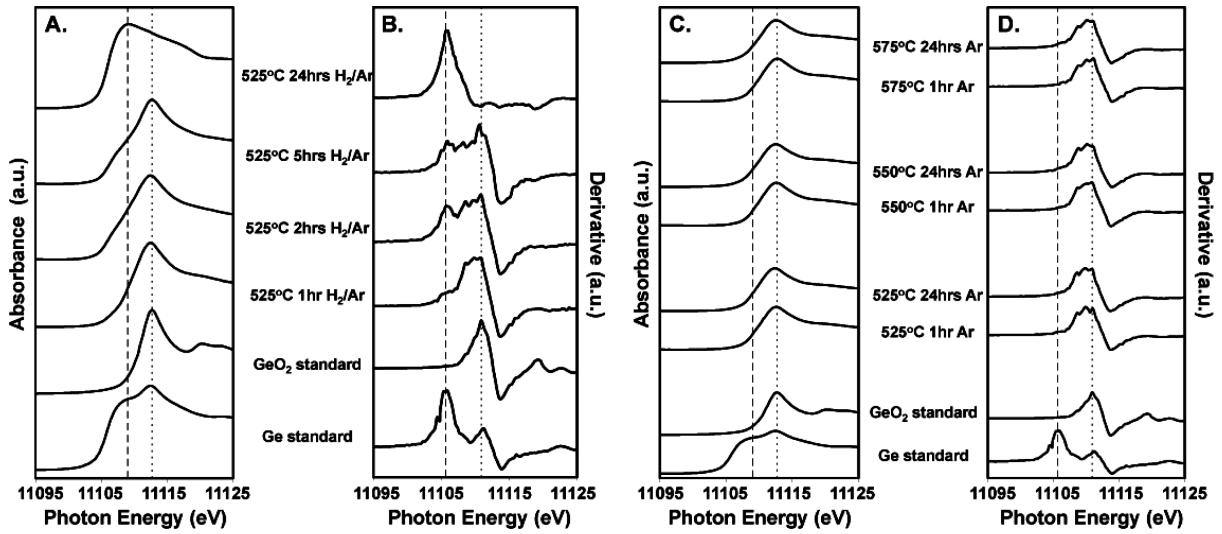

Figure 3. (A) NEXAFS spectra at the Ge K-edge showing the effect of thermal processing time of $(C_6H_5GeO_{1.5})_n$ at 525 °C under 5% H_2/95% Ar. (B) Derivative plot of the NEXAFS spectra. (C) NEXAFS spectra at the Ge K-edge showing the effect of thermal processing time of $(C_6H_5GeO_{1.5})_n$ at 525, 550, and 575 °C under 100% Ar. (D) Derivative plot of the NEXAFS spectra. Vertical lines are provided to show the peak energies for Ge (---) and GeO_2 (· · ·) standards.

similar materials, including amorphous GeO_x films and Ge nanowires,[33,41,42] the Ge 3d region is routinely fit to the Ge $3d_{5/2}$ and Ge $3d_{3/2}$ partner lines for $Ge^{(0)}$ and to low-valent intermediate Ge oxides (i.e., $Ge^{(n)}$; n = I, II, III, and IV for Ge_2O, GeO, Ge_2O_3, and GeO_2, respectively). The noncrystalline nature of these Ge oxides in the present systems affords a distribution of Ge chemical and electronic environments that broaden XP peaks and make spin−orbit partner line assignments nontrivial.[43] As seen in Figure 2, after processing at 600 °C in 100% Ar, the XP spectrum is dominated by $Ge^{(IV)}$ and $Ge^{(III)}$ species, with smaller contributions from lower valent oxide species and $Ge^{(0)}$. This agrees with our proposal regarding the onset of the redistribution reactions at $T >$ 500 °C (vide supra). The high concentration of $Ge^{(IV)}$ relative to other oxide species can be attributed to the formation of GeO_2 during all steps of the redistribution reactions (eq 1). Increasing the processing temperature to 650 °C results in a relative increase in $Ge^{(II)}$ and $Ge^{(0)}$ species, consistent with continued redistribution chemistry. Further increasing the temperature to 700 °C results in a significant increase in the relative intensities of $Ge^{(IV)}$, $Ge^{(II)}$, and $Ge^{(0)}$, again as a result of the continuing redistribution reactions.

In comparison, the Ge 3d region of the XP spectrum for $(C_6H_5GeO_{1.5})_n$ processed at 600 °C in 5% H_2/95% Ar is presented in Figure 2D. It is clear that when $(C_6H_5GeO_{1.5})_n$ is processed in the presence of hydrogen, $Ge^{(IV)}$ is the dominant oxide species, and there is a substantial increase in the relative amount of $Ge^{(0)}$ compared to equivalent samples processed in 100% Ar. The low relative concentration of low-valent intermediate Ge oxides can be attributed to their preferential reduction by the H_2-containing atmosphere (eq 2), which also accounts for the greater concentration of $Ge^{(0)}$. Again, it is clear from these XP results that processing atmosphere composition directly and dramatically influences the evolution of Ge-NCs by affecting the concentration of Ge species present in the thermally treated GRO.

We have previously observed that varying thermal processing time is an effective method for controlling Ge-NC diameter when processed in 5% H_2/95% Ar.[21] To further investigate this effect, the role of processing atmosphere was investigated in the formation and growth of Ge-NCs from $(C_6H_5GeO_{1.5})_n$ as a function of varying the processing time. Figure 3A shows the normalized NEXAFS spectra at the Ge K-edge for samples of $(C_6H_5GeO_{1.5})_n$ thermally processed at 525 °C under 5% H_2/95% Ar for 1, 2, 5, and 24 h. With increased processing time, it is clear the intensity of the $Ge^{(0)}$ absorption feature at ca. 11109 eV increases with respect to the $Ge^{(IV)}$ absorption. This trend is also evident in the derivative plot (Figure 3B). These observations are consistent with the reduction of the Ge oxide species, including the fully oxidized GeO_2 matrix, by the H_2-containing processing atmosphere.

Figure 3C shows the normalized NEXAFS spectra at the Ge K-edge for samples of $(C_6H_5GeO_{1.5})_n$ thermally processed at 525, 550, and 575 °C, for 1 and 24 h in 100% Ar. These conditions were chosen to provide a direct comparison to the samples shown in Figure 3A. Again, the effect of processing atmosphere is marked. Prolonged heating at 525 °C (i.e., 1 h versus 24 h) results in no detectable changes to the spectral characteristics, in contrast to what was observed under 5% H_2/95% Ar. Furthermore, even prolonged processing at 550 and 575 °C did not appreciably change the absorption spectra. The derivative plots (Figure 3D) also do not show any change with extended processing time.

To verify if spectral changes could result from extended thermal processing in a 100% Ar atmosphere for samples

(41) Molle, A.; Bhuiyan, M. N. K.; Tallarida, G.; Fanciulli, M. *Mater. Sci. Semicond. Process.* **2006**, *9*, 673.
(42) Adhikari, H.; McIntyre, P. C.; Sun, S.; Pianetta, P.; Chidsey, C. E. D. *Appl. Phys. Lett.* **2005**, *87*, 263109.
(43) Zanatta, A. R.; Chambouleyron, I. *Phys. Status Solidi B* **1996**, *193*, 399.

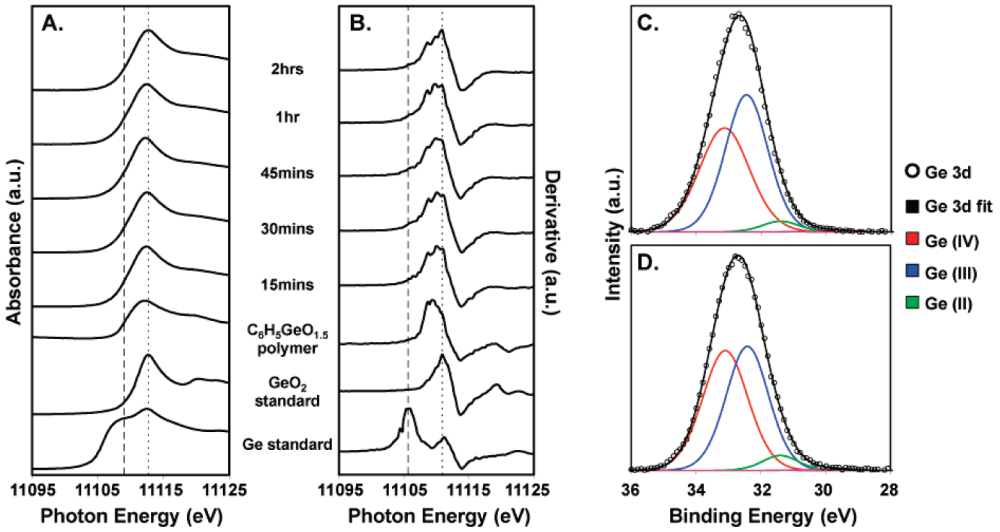

Figure 4. (A) NEXAFS spectra at the Ge K-edge showing the effect of thermal processing time of $(C_6H_5GeO_{1.5})_n$ at 650 °C in 100% Ar. (B) Derivative plot of the NEXAFS spectra. Vertical lines are provided to show the peak energies for Ge (---) and GeO_2 (· · ·) standards. (C) High-resolution XP spectrum of the Ge 3d spectral region for samples processed at 650 °C for 15 min in 100% Ar. (D) High-resolution XP spectrum of the Ge 3d spectral region for samples processed at 650 °C for 2 h in 100% Ar.

in which $Ge^{(0)}$ was known to be present, the effect of processing time was monitored at 650 °C for 15 min, 30 min, 45 min, 1 h, and 2 h. Recall, the presence of $Ge^{(0)}$ was established upon processing at 650 °C for 1 h under 100% Ar (Figure 1C). Figure 4A shows the normalized NEXAFS spectra at the Ge K-edge for these samples. It is clear that no appreciable variation in the amount of $Ge^{(0)}$ results with prolonged processing under these conditions, as is also evident in the derivative plot (Figure 4B). However, analysis of the Ge 3d region of the XP spectrum (Figures 4C,D) shows that extending the processing time from 15 min (C) to 2 h (D) results in a relative increase in the amount of $Ge^{(IV)}$ and $Ge^{(II)}$ with respect to $Ge^{(III)}$. This observation is indicative of continued redistribution reactions as described in eq 1. However, there was no noticeable change in lower valent Ge species, including $Ge^{(0)}$. These observations may be attributed to kinetic barriers associated with the diffusion of Ge atoms produced through the redistribution chemistry. This is consistent with previous trends that showed no change in crystal size in Si-NCs produced from SRO networks with extended processing time.[5] Therefore, although the redistribution chemistry is occurring, kinetic factors appear to inhibit cluster growth by limiting Ge atomic diffusion. In contrast, in 5% H_2/95% Ar, reduction of Ge oxide species has been reported to allow greater diffusion of Ge atoms and additional NC growth with extended thermal processing.[29]

The emerging picture at this point is processing atmosphere governs the distribution of Ge species, both oxidized and elemental, by influencing the contributions from redistribution and reduction reactions of the GRO. In doing so, the concentration of elemental Ge and the diffusion of Ge atoms throughout the matrix are impacted. In addition to monitoring changes in the Ge electronic characteristics, further insight into the influence of processing atmosphere on the formation and growth of Ge-NCs was obtained by X-ray diffraction (XRD). The onset and evolution of crystallinity is crucial to the detailed understanding of the optical and electronic properties of the system (vide infra). Figure 5A shows the evolution of the XRD pattern for samples processed in 100% Ar as a function of peak processing temperature, in which the emergence of reflections characteristic of diamond structure Ge occurs at 600 °C. This is consistent with NEXAFS and XP spectroscopy showing the emergence of $Ge^{(0)}$ at similar temperatures (vide supra). Higher processing temperature results in an intensity increase of these reflections, suggestive of either improved crystallinity (i.e., annealing of defects)[5] or a higher population of crystalline domains. Surprisingly, no change in the breadth of the reflections is observed with increased processing temperature, indicative of little or no change in domain size. In fact, Scherrer analysis of XRD peak broadening provided a mean Ge-NC diameter of ca. 20 nm for all samples, suggesting variations in peak processing temperature do not afford a viable experimental method for controlling the size of Ge-NCs produced by the thermal processing of $(C_6H_5GeO_{1.5})_n$ in 100% Ar atmosphere.

Figure 5B shows the evolution of crystallinity with processing time at 650 °C under 100% Ar. It is clear that extended thermal processing does not affect the crystallinity of the samples substantially. There is no appreciable change in the intensity of the Ge reflections, nor is there a change in the breadth of the reflections. The slight decrease in the intensity of the reflections for samples processed for 2 h likely arises from Ge evaporation, as supported by TGA (vide supra). Again, highlighting that varying processing time is not a suitable method for controlling Ge-NC size in 100% Ar. In contrast, in 5% H_2/95% Ar crystalline Ge emerges for samples processed at 525 °C, and increased processing temperature results in narrowing of these Ge reflections, an increase in their intensity, and emergence of higher order crystal planes, all consistent with NC growth. Furthermore, prolonged

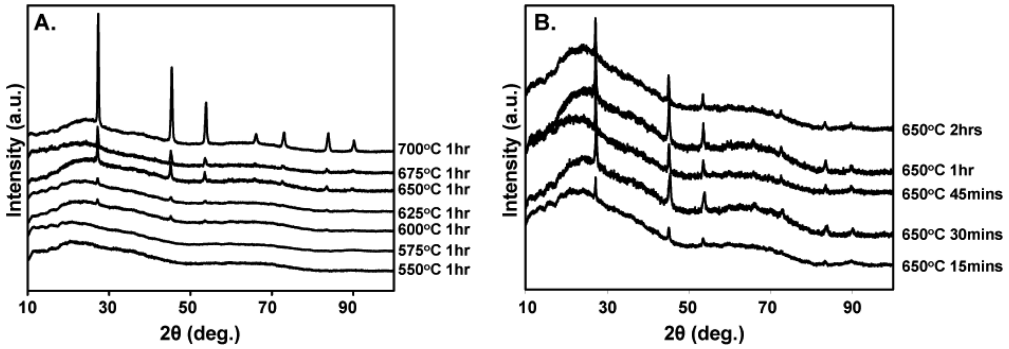

Figure 5. (A) XRD pattern showing the effect of processing temperature on the crystallinity of Ge-NCs processed in 100% Ar. (B) XRD pattern showing the effect of processing time on the crystallinity of Ge-NCs processed in 100% Ar.

heating at 525 °C in 5% H_2/95% Ar also results in NC growth.[21] Therefore, thermal processing in slightly reducing atmospheres is a straightforward and convenient method by which to control Ge-NC diameter. These observations are clearly indicative of the important role of processing atmosphere composition in the formation and evolution of Ge-NCs from $(C_6H_5GeO_{1.5})_n$.

Discussion

Processing atmosphere composition is a very important parameter in the formation and growth of GeO_2-embedded Ge-NCs produced from $(C_6H_5GeO_{1.5})_n$. These conclusions are also applicable to GROs formed by other experimental means. Through its influence on the thermally driven chemical reactions that transform the GRO network, not only are additional $Ge^{(0)}$ formation pathways made available but also secondary effects present themselves, in particular the diffusion of Ge through the oxide matrix. In 100% Ar, only redistribution reactions (eq 1) can take place. The extent of these reactions can be appreciated by considering the spectroscopic data presented herein. NEXAFS and XP spectroscopy suggest the formation of GeO_2 at $T = 525$ °C, which is possible only through these reactions. However, this characterization also demonstrates the formation of elemental Ge at T ≥ 600 °C. Even prolonged heating (i.e., 24 h) at 525, 550, and 575 °C did not result in any discernible $Ge^{(0)}$ signature. This observation suggests that although the redistribution chemistry is initiated at ca. 525 °C, the thermal energy supplied is not sufficient to form elemental Ge clusters, likely the result of energetic requirements associated with solid state diffusion of Ge atoms through a dense matrix. In 5% H_2/95% Ar, the reduction of Ge oxides "opens up" the matrix,[29] allowing greater Ge diffusion and ultimately to the production of Ge-NCs at lower temperatures (i.e., 525 °C). With increasing temperature and/or processing time, this allows for Ge-NC growth and offers the possibility of nanocrystal size control.

It is interesting to consider that in 100% Ar, no change in Ge-NC size is observed with changes to peak processing temperature or time. We have already established that, under these conditions, a greater energetic barrier to diffusion through the denser oxide matrix, together with an overall lower concentration of elemental Ge, results in $Ge^{(0)}$ clustering and crystallization at higher temperatures. The fact that no additional crystal growth is observed with increased processing temperatures could be the result of a depleted feedstock of $Ge^{(0)}$ because of the complete "disproportionation" of the GRO (i.e., $4GeO_{1.5} \rightarrow Ge + 3GeO_2$). The high relative concentrations of $Ge^{(III)}$, $Ge^{(II)}$, and $Ge^{(I)}$ in the XP spectra for samples processed at 600 and 650 °C would seem to discount this proposal, as additional Ge could be produced from the reactions in eq 1. However, these same species have been shown to be the dominant surface oxides in other Ge nanostructures[42] and, therefore, could be interfacial oxides bridging the Ge-NCs and GeO_2 matrix in the present system. Another possibility may be the influence of the bonding density mismatch between the Ge-NC surface and surrounding oxide matrix. Reports on SiO_2-embedded Si-NCs have postulated that for oxide-embedded nanocrystals, this mismatch forces the elemental clusters to adopt a convex shape and remain small in order to minimize interfacial strain.[44] In such a manner, additional growth of Ge-NCs could be hindered. Recent investigations have also reported increased stress development in SiO_2-embedded Ge-NCs with processing temperature resulting from nanocrystal/matrix interactions. With high temperatures (900−1000 °C), this stress was relieved with the out-diffusion of Ge atoms, and no additional nanocrystal growth was observed.[27,29] With these considerations, for the present system, increasing temperature causes additional Ge-NCs to be formed rather than contribute to the growth of existing nanocrystals in order to minimize the stress imposed by the matrix. Nevertheless, it can be concluded that thermal processing of $(C_6H_5GeO_{1.5})_n$ in an inert atmosphere is not an effective method for controlling Ge-NC size. That said, compositional tuning of $(C_6H_5GeO_x)_n$ may prove to be effective in producing size-controlled Ge-NCs, exploiting the size invariance of the present Ar atmosphere processing to achieve very narrow size distributions.

Conclusion

We have demonstrated the effect of processing atmosphere (5% H_2/95% Ar vs 100% Ar) on the evolution of

(44) Hohl, A.; Wieder, T.; Van Aken, P. A.; Weirich, T. E.; Denninger, G.; Vidal, M.; Oswald, S.; Deneke, C.; Mayer, J.; Fuess, H. *J. Non-Cryst. Solids* **2003**, *320*, 255.

GeO_2-embedded Ge-NCs produced from the thermal processing of $(C_6H_5GeO_{1.5})_n$ derived from phenyl trichlorogermane. While no effect was observed in the initial pyrolytic liberation of the phenyl groups, the influence of processing atmosphere on subsequent thermally induced chemical transformations of the GRO network was pronounced. In an inert Ar atmosphere, redistribution chemistry (disproportionation) generated 20 nm Ge-NCs at 600 °C, and variations to peak processing temperature and time did not afford nanocrystal size tuning. In contrast, the presence of hydrogen in the processing atmosphere not only allows redistribution chemistry but also allows chemical reduction of germanium oxide species. As such, nanocrystal formation is seen at lower temperature (525 °C), and variations to processing temperature and time were found to be effective methods to tailor Ge-NC size.

Acknowledgment. The authors acknowledge funding from the Natural Sciences and Engineering Research Council of Canada (NSERC), Canada Foundation for Innovation (CFI), Alberta Science and Research Investment Program (ASRIP), and University of Alberta Department of Chemistry. C. W. Moffat and R. Lister are thanked for assistance with TGA. The staff of the Alberta Centre for Surface Engineering and Sciences (ACSES) are thanked for XPS analysis. PNC/XOR facilities at the Advanced Photon Source and research at these facilities are supported by the US Department of Energy-Basic Energy Sciences, a major facilities access grant from NSERC, the University of Washington, Simon Fraser University, and the Advanced Photon Source. Use of the Advanced Photon Source is also supported by the U.S. Department of Energy, Office of Science, Office of Basic Energy Sciences, under Contract DE-AC02-06CH11357. Robert A. Gordon is thanked for assistance with NEXAFS spectroscopy. J. A. Kelly, S. L. McFarlane, and T. Telesco are thanked for useful discussions.

Supporting Information Available: XP spectrum of unprocessed $(C_6H_5GeO_{1.5})_n$ (PDF). This material is available free of charge via the Internet at http://pubs.acs.org.